

Merger Dynamics of the Pair of Galaxy Clusters — A399 and A401 *

Qi-Rong Yuan^{1,2}, Peng-Fei Yan³, Yan-Bin Yang² and Xu Zhou²

¹ Department of Physics, Nanjing Normal University, Nanjing 210097
yuanqirong@njnu.edu.cn

² National Astronomical Observatories, Chinese Academy of Sciences, Beijing 100012

³ Department of Mathematics and Physics, Qingdao University of Science and Technology,
Qingdao 266042

Received 2004 July 15; accepted 2005 February 21

Abstract Convincing evidence for a past interaction between the two rich clusters A399 and A401 was recently found in the X-ray imaging observations. We examine the structure and dynamics of this pair of galaxy clusters. A mixture-modeling algorithm was applied to obtain a robust partition into two clusters, which allowed us to discuss the virial mass and velocity distribution of each cluster. Assuming that these two clusters follow a linear orbit and they have once experienced a close encounter, we model the binary cluster as a two-body system. As a result, four gravitationally bound solutions are obtained. The recent X-ray observations seem to favor a scenario in which the two clusters with a true separation of $5.4h^{-1}$ Mpc are currently expanding at 583 km s^{-1} along a direction with a projection angle of 67.5° , and they will reach a maximum extent of $5.65 h^{-1}$ Mpc in about $1.0 h^{-1}$ Gyr.

Key words: galaxies: clusters: individual (A399, A401) — galaxies: kinematics and dynamics

1 INTRODUCTION

According to the hierarchical bottom-up scenario, clusters of galaxies are thought to be formed by accreting and merging of subunits. The structure and dynamics of those rich galaxy clusters with ongoing merger events are of great importance for understanding the cluster evolution. N-body numeric simulations show that substructure may occur in individual rich clusters before their final collapse and virialization (White 1976; Burns et al. 1994). Since the cluster merging events are the most common and energetic phenomena in the Universe, more and more observational efforts in optical and X-ray bands have been devoted to nearby rich clusters with

* Supported by the National Natural Science Foundation of China.

significant substructures (e.g., White, Briel & Henry 1993; Gastaldello et al. 2003). When these subsystems are sufficiently separated they may be classified as separate galaxy clusters. The interacting system of clusters A399 and A401 is a good example. They have long been treated as a merging pair of clusters since they are close to each other, with a projected separation of $\sim 0.6^\circ$ between their central cD galaxies (McGlynn & Fabian 1984; Oegerle & Hill 1994). The temperature map for this binary cluster, derived from the *ASCA* spatially resolved spectroscopic data, suggests a possible physical link or a massive dark matter filament between these two clusters (Markevitch et al. 1998). X-ray observation with the *ROSAT* High Resolution Imager (HRI) unveiled a significant linear structure of A399 pointing directly to the core of A401, and this feature might be resulted from a past violent interaction (Fabian, Peres & White 1997). Recent *XMM-Newton* observations also confirmed the enhanced X-ray flux and temperature in the region between the two clusters (Sakelliou & Ponman 2004).

Therefore, it is of great interest to search for the optical anomalies in dynamics of the member galaxies. In general, the merger history can be modelled on the basis of the structure and dynamics of the cluster galaxies, intracluster gas, and intergalactic medium (e.g., Colless & Dunn 1996). This paper will use existing redshift measurements to investigate possible structures in the 2-dimension map and in velocity space. A widely known mixture-modeling algorithm, known as the KMM algorithm (Ashman et al. 1994), will be applied to obtain a robust separation of these two clusters. Disregarding the rotation of the system, we will try to model this cluster pair as a two-body system on the basis of the velocity distribution and virial mass estimates. In Sect. 2, we present the spatial distribution and localized variations in the velocity distribution for all the member galaxies in the A399/A401 system as a whole. We apply the KMM partition algorithm and discuss the velocity distribution for each cluster in Sect. 3. Then, a virial mass estimate and a two-body modeling for this binary system of galaxy clusters are made in Sect. 4. Finally, a summary is given in Sect. 5.

2 PROPERTIES OF THE SAMPLE

A399 and A401 are nearby clusters of galaxies ($z \sim 0.07181$ and 0.07366 , Oegerle & Hill 2001), classified respectively as type I-II and I clusters by Bautz & Morgan (1970). With respect to the center of this binary system ($2^{\text{h}}58^{\text{m}}30^{\text{s}}, +13^\circ 20''$; J2000.0), 1331 extragalactic objects with positional offsets less than 100.0 arcmin were extracted from the NASA/IPAC Extragalactic Database (NED). However, only 240 galaxies have spectroscopic redshifts. The remainder appears only in one of the imaging surveys from radio, infrared, and X-ray wavebands.

Most of the spectroscopic data were contributed by Hill & Oegerle (1993) who carried out a survey of cD clusters. The redshift measurements were detailed in Hill & Oegerle (1993), and typical velocity uncertainty for the galaxies is less than 100 km s^{-1} . The distribution of spectroscopic redshifts for the 240 known galaxies is shown in Fig. 1. There are 215 galaxies with redshifts in the range $18000 \text{ km s}^{-1} < cz < 25000 \text{ km s}^{-1}$, with a peak at $\sim 21500 \text{ km s}^{-1}$. Only one peak can be found in the velocity distribution because the velocity dispersions for individual clusters are larger than the apparent velocity separation between two clusters. There is no ambiguity in treating these 215 galaxies as members of this cluster pair since the redshift distribution is quite concentrated and isolated: contamination from foreground and background galaxies should be very slight. The spatial distribution for these 215 galaxies is presented in Fig. 2. We superpose on it the contour map of the surface density smoothed by a Gaussian window with $\sigma = 2'$. Because of the severe overlap in their redshift distributions, clusters A399 and A401 can not be completely resolved by the velocity distribution only.

In order to detect the substructures in both the velocity space and the projected map, we make use of the κ -test (Colless & Dunn 1996) for the A399/A401 system as a whole. The statistic κ_n is defined to characterize the local deviation on the scale of groups of n nearest neighbors. A larger κ_n means a greater probability that the local velocity distribution differs from the overall distribution. The probability that κ_n is larger than the observed value κ_n^{obs} , $P(\kappa_n > \kappa_n^{\text{obs}})$, can be estimated by Monte Carlo simulations with randomly shuffling velocities. Table 1 gives the results of κ -test for the 215 known member galaxies, and 10^3 simulations were used to estimate $P(\kappa_n > \kappa_n^{\text{obs}})$ in all cases.

Table 1 Result of κ -Test for 215 Member Galaxies in the Binary System

n	4	5	6	7	8	9	10	11	12
$P(\kappa_n > \kappa_n^{\text{obs}})$	18.3%	44.4%	42.6%	34.1%	17.0%	11.9%	6.8%	15.1%	14.5%

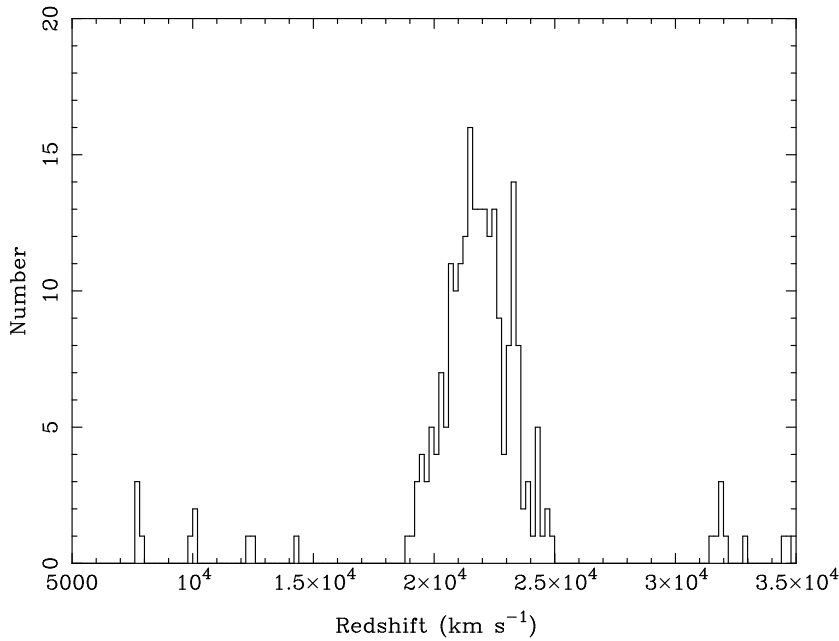


Fig. 1 Distribution of the radial velocities for 240 galaxies with known spectroscopic redshifts. The bin size is 1000 km s^{-1} .

It is found that the optimum scale of the nearest neighbors is 10, and the substructure appears most obvious on this scale. The bubble plot in Fig. 3 shows the location of localized variation using neighbor size $n = 10$, and the bubble size for each galaxy is proportional to $-\log[P_{\text{KS}}(D > D_{\text{obs}})]$. Therefore, larger bubbles indicate a greater difference between the local and overall velocity distributions. A comparison with Fig. 2 shows that the bubble clusterings near the central regions of A399 and A401 are significant, which indicates a distinct difference between the localized and whole velocity distributions.

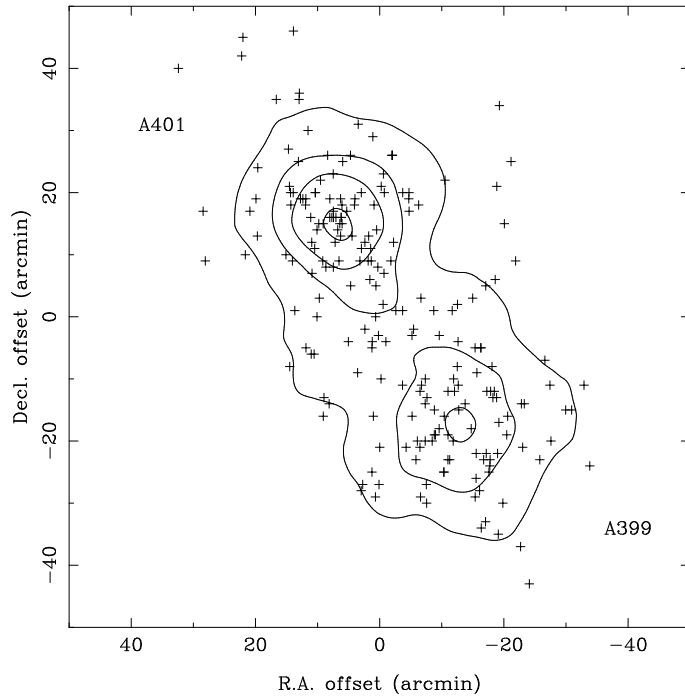


Fig. 2 Spatial distribution for 215 member galaxies of the binary system of galaxy clusters, superposed by the contour map of the surface density where the smoothing Gaussian window with a radius of $2'$ is used. The contour levels are $0.03, 0.09, 0.15,$ and 0.21 arcmin^{-2} , respectively.

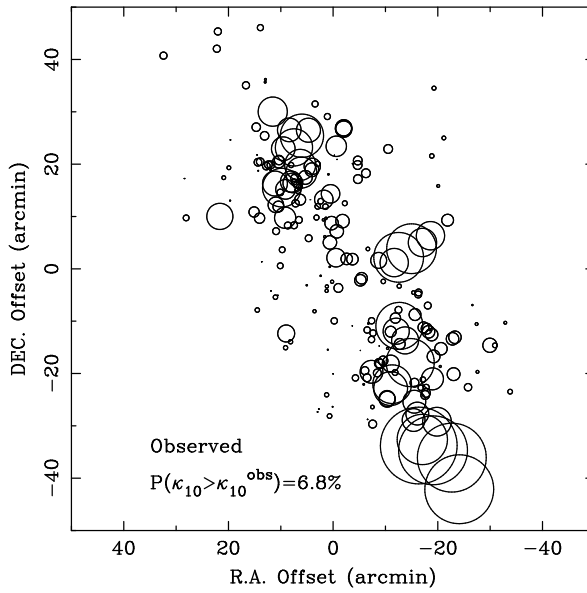


Fig. 3 Bubble plot showing the degree of difference between the local velocity distribution for groups of 10 nearest neighbors and the overall distribution of 215 known cluster galaxies.

3 THE KMM PARTITION INTO TWO CLUSTERS

For studying the dynamical properties for each cluster, those 215 galaxies should be correctly partitioned. It is relatively easy to partition the galaxies whose projected locations appear close to the cluster centers. However, for the galaxies located halfway between the cluster centers, the partition might become a rather ambiguous task.

In order to achieve a robust partition, we apply a currently favored technique of mixture modeling, namely the KMM algorithm, on the sample of 215 galaxies. The KMM is a maximum-likelihood algorithm which assigns objects into groups and assesses the improvement in fitting a multi-group model over a single group model (Ashman et al. 1994). A detailed description of the KMM algorithm can be found, e.g., in Nemeč & Nemeč (1993). For a dynamically relaxed cluster, the line-of-sight velocities of galaxies are expected to be Gaussian distributed. Since A399 and A401 are two gravitationally distinct clusters of galaxies, we here apply the KMM algorithm which estimates the statistical significance of bimodality based on the three-dimension data: the projected positions of the galaxies and the radial velocity, just as Colless & Dunn (1996) did. When an initial partition into two clusters or a set of initial parameters for each cluster is given, the KMM algorithm can start iterating toward the maximum-likelihood solution. Table 2 lists the various initial partitions/parameters that we used and the corresponding final solutions, where $(\bar{x}_1, \bar{y}_1, \bar{v}_1)$ and $(\bar{x}_2, \bar{y}_2, \bar{v}_2)$ are the mean positions and velocities of A401 and A399, respectively, $(\sigma_{x_1}, \sigma_{y_1}, \sigma_{v_1})$ and $(\sigma_{x_2}, \sigma_{y_2}, \sigma_{v_2})$ are their standard deviations in positions and velocities, and f_1 and f_2 are the fractions of the sample in the two clusters. Also listed is the estimated overall correction rate given by the KMM algorithm.

Table 2 Initial Parameters and Final Solutions of the KMM Algorithm

Case	$(\bar{x}_1, \bar{y}_1, \bar{v}_1)$	$(\sigma_{x_1}, \sigma_{y_1}, \sigma_{v_1})$	$(\bar{x}_2, \bar{y}_2, \bar{v}_2)$	$(\sigma_{x_2}, \sigma_{y_2}, \sigma_{v_2})$	(f_1, f_2)	Rate
Initial Parameters						
1	(5.9, 16.9, 22133)	(9.8, 9.9, 1208)	(-11.4, -15.7, 21536)	(9.8, 9.5, 1227)	(0.521, 0.479)	
2	(4.0, 14.6, 22080)	(10.7, 11.1, 1212)	(-11.7, -18.3, 21505)	(10.3, 7.7, 1234)	(0.595, 0.405)	
3	(5.0, 16.8, 22126)	(10.5, 9.7, 1204)	(-9.0, -18.1, 21378)	(10.4, 8.9, 1232)	(0.530, 0.470)	
Final Solutions						
1	(4.8, 14.4, 22107)	(10.2, 11.7, 1185)	(-12.6, -17.4, 21477)	(9.1, 8.8, 1241)	(0.586, 0.414)	95.2%
2	(4.9, 14.5, 22107)	(10.2, 11.7, 1185)	(-12.6, -17.3, 21477)	(9.2, 8.9, 1240)	(0.585, 0.415)	95.2%
3	(4.8, 14.4, 22107)	(10.2, 11.7, 1185)	(-12.6, -17.4, 21477)	(9.1, 8.8, 1241)	(0.587, 0.413)	95.1%

We consider first two cases. In cases 1, we chose to specify the initial positions and dispersions of the two clusters, while in case 2 we simply make a partition of the sample, assigning to A401 all galaxies with declination offset $y > -5$ arcmin. For each case, the KMM algorithm searched for an optimum two-group solution, and converged to a very similar result. The estimate of the correct allocation rate reached 95%. In a third case, case 3, we used a different partition: we assign to A399 all galaxies within an angular distance of 20 arcmin of the central cD galaxy UGC 2438. We obtained the same final solution.

According to the final partition into two clusters, there are 127 galaxies belonging to A401, and 88 galaxies to A399. The spatial distribution for each cluster is plotted in Fig. 4a. Then, we apply the κ -tests again for the individual clusters, and the probability $P(\kappa_n > \kappa_n^{\text{obs}})$ is estimated for each cluster. Table 3 presents the κ -test results, and the corresponding bubble plot are given

in Fig. 4b. Compared with the last κ -test on the whole binary system (see Table 1 and Fig. 3), the variation of localized velocity distribution for each cluster is significantly smaller, which indicates that the KMM algorithm has arrived at a robust partition.

Table 3 Results of κ -tests for 88 Galaxies in A399 and for 127 Galaxies in A401

Group size n	2	3	4	5	6	7	8
$P(\kappa_n > \kappa_n^{\text{obs}})$ for A399	33.5%	8.7%	17.5%	56.7%	52.7%	57.1%	59.1%
$P(\kappa_n > \kappa_n^{\text{obs}})$ for A401	7.9%	59.4%	59.0%	87.3%	93.1%	87.6%	72.0%

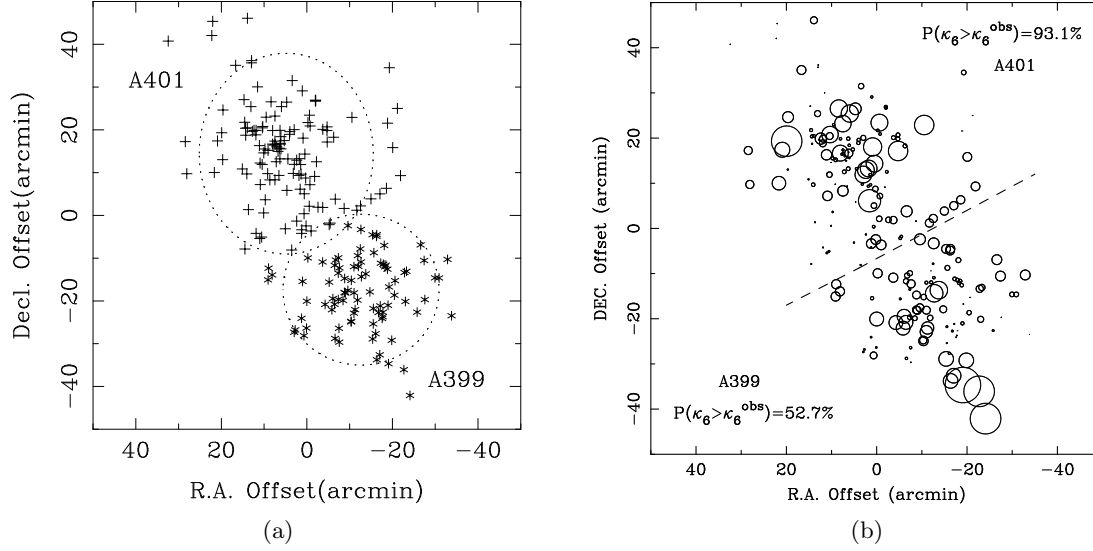


Fig. 4 (a) Projected positions for the member galaxies of A399 (denoted by asterisks) and of A401 (denoted by plus sign). The dotted ellipses are the 2σ contours of the fitted Gaussians. (b) Bubble plots for groups of six nearest neighbors for 127 galaxies in A401 and 88 galaxies in A399. The dashed line separates the two clusters.

4 MERGER DYNAMICS BETWEEN A399 AND A401

4.1 Velocity Structure

The radial velocity distributions for the binary system and each cluster are given in Fig. 5. The solid lines represent the best-fit Gaussians with the mean velocities and dispersions listed in Table 2. To characterize the kinematical properties of clusters of galaxies, two robust estimators analogous to the velocity mean and standard deviation, namely the biweight location (C_{BI}) and scale (S_{BI}), were defined by Beers et al. (1990). These two quantities are insensitive to outliers, and robust for a broad range of probable non-Gaussian underlying populations. Using the *ROSTAT* software, we compute the biweight location and scale in the line-of-sight velocity distribution for each cluster, and we obtain $C_{\text{BI}} = 21491 \pm 141 \text{ km s}^{-1}$ and $S_{\text{BI}} = 1315 \pm 82 \text{ km s}^{-1}$ for A399, and $C_{\text{BI}} = 22069 \pm 107 \text{ km s}^{-1}$ and $S_{\text{BI}} = 1212 \pm 71 \text{ km s}^{-1}$ for A401. The physical line-of-sight velocity difference between the two clusters is $V_r = \Delta(C_{\text{BI}})/(1 + \bar{z}) = 539 \pm 165 \text{ km s}^{-1}$.

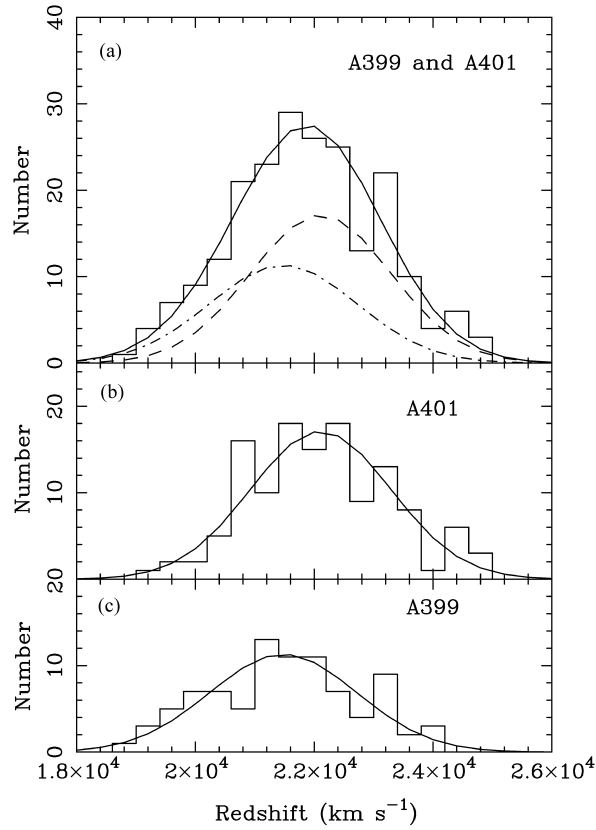


Fig. 5 Velocity distributions for the galaxies in (a) the entire binary system, (b) A401, and (c) A399, superposed with the fitted Gaussians.

4.2 Virial Mass Estimate

A399 and A401 are gravitationally bound to each other. In order to determine the dynamical state of the binary system, we will apply the virial theorem for estimating the mass of each cluster. Assuming that the cluster is bound and the galaxy orbits are random, the virial mass (M_{vt}) can be estimated from the following standard formula (Geller & Peebles 1973; Oegerle & Hill 1994):

$$M_{\text{vt}} = \frac{3\pi}{G} \sigma_r^2 D N_p \left(\sum_{i>j} \frac{1}{\theta_{ij}} \right),$$

where σ_r is the line-of-sight velocity dispersion, D is the cosmological distance of the cluster, $N_p = N(N-1)/2$ is the number of galaxy pairs, and θ_{ij} is the angular separation between galaxies i and j . The extended X-ray emission associated with A399 and A401, revealed by the *ROSAT* HRI imaging observations (Fabian et al. 1997), indicates that at least the first of these assumptions is reasonable. We derive the virial masses of $2.0h^{-1} \times 10^{15} M_\odot$ and $2.1h^{-1} \times 10^{15} M_\odot$ for A399 and A401, respectively.

4.3 Two-Body Models

With the estimated mass for each cluster, we can investigate the state of evolution. A concise dynamical model for this binary system is the two-body model which was first applied to clusters by Beers, Geller & Huchra (1982). In this model two clusters are treated as point masses following a linear orbit under their mutual gravity. They are presumed to have started with zero separation and then to have moved apart before turning around. Given the projected separation of this binary system R_p , the relative radial velocity V_r and the total mass M , the model can speculate on the projection angle α (the angle between the line joining the two clusters and the plane of the sky), the true separation R , and relative velocity V . The equations of motion are:

$$V = \frac{V_r}{\sin \alpha} = \left(\frac{2GM}{R_m} \right)^{1/2} \frac{\sin \chi}{(1 - \cos \chi)}, \quad (1)$$

$$R = \frac{R_p}{\cos \alpha} = \frac{R_m}{2}(1 - \cos \chi), \quad (2)$$

$$t = t_0 = \left(\frac{R_m^3}{8GM} \right)^{1/2} (\chi - \sin \chi), \quad (3)$$

where R_m is the maximum expansion, M is the total mass of the binary system, t_0 is the age of the universe, and χ is the angle tracing the merger process. The two clusters have zero separation when $\chi = 0, 2\pi$, while they are at maximum expansion when $\chi = \pi, 3\pi$. Due to the ambiguity in observing the system only in projection, this model usually results in more than one orbital solution.

The KMM analysis provides the initial estimate of the projected separation R_p of the two-body model. Assuming a Friedmann-Robertson-Walker cosmology with $\Omega_m = 0.3$, $\Omega_\Lambda = 0.7$, we adopt the age of the universe as $t_0 = 9.43 h^{-1} \text{Gyr} = 2.976 h^{-1} \times 10^{17} \text{s}$, and the angular separation between the centroids of these two clusters (~ 36.3 arcmin) corresponds to a projected distance R_p of $2.05 h^{-1} \text{Mpc}$ at the average redshift. We take the total mass $M = \sum M_{vt} = 4.1 h^{-1} \times 10^{15} M_\odot$ in our modeling.

Previous applications of the two-body models tried to solve the dynamical solutions within a range of $0 < \chi < 2\pi$, assuming that the subclusters start to separate at $t = 0$ and are moving apart or coming together for the first time in their history (Beers, Geller & Huchra 1982; Oegerle & Hill 1994; Colless & Dunn 1996). However, numerical simulations of cluster collisions by McGlynn & Fabian (1984) showed that clusters can even pass through each other without destroying the optical components. For this pair of clusters, recent observational evidence in X-ray and radio bands supports a picture in which A399 and A400 have passed through each other in the past. As mentioned in Sect. 1, Fabian et al. (1997) found a linear X-ray structure in A399 pointing at the cD galaxy of A401, indicating a past violent interaction. On the other hand, the absence of a cooling flows in both A399 and A401 was first found by Edge et al. (1992), and confirmed by Markevitch et al. (1998) and Sakelliou & Ponman (2004). According to the numerical experiments of McGlynn & Fabian (1984), the structure of a cooling flow can be disrupted by the merger of two similar clusters. A simulations by Burns et al. (1997) showed that mergers of clusters with a mass ratio of 1:4 may destroy a pre-existing cooling flow. The picture of a previous interaction between these clusters is also supported by the temperature map for this system which shows a bridge of matter between the clusters (Markevitch et al. 1998). Furthermore, an extensive cluster radio halo is found to be associated with A401, suggesting the coalescence of clusters (Harris et al. 1980).

Based on the above observations, we suppose that the two clusters started at $t = 0$ with zero separation, expanded to a maximum extent, and experienced one close encounter; this would mean a χ range from 2π to 4π . From the equations of motion given above, four two-body models are allowed within $2\pi < \chi < 4\pi$, including two expanding (outgoing) and two collapsing (incoming) models. Figure 6 shows the (α, V_r) -plane where four solutions at $V_r = 539 \pm 165$ km s $^{-1}$ are found in the bound region. Figure 6 also shows the limiting curve for the bound region, defined by the Newtonian criterion $V_r^2 R_p \leq 2GM \sin^2 \alpha \cos \alpha$. Meanwhile, we derive three solutions within $0 < \chi < 2\pi$ for reference only. The seven solutions are presented in Table 4.

Table 4 Gravitationally Bound Solutions for the Two-body Model

Case	Dynamical Status	χ (π rad.)	α (degree)	V (km s $^{-1}$)	R (h^{-1} Mpc)	R_m (h^{-1} Mpc)
(a)	Outgoing	0.776	$81.6^{+0.6}_{-0.6}$	545^{+165}_{-166}	$14.09^{+1.04}_{-1.00}$	$15.99^{+3.32}_{-2.16}$
(b)	Incoming	1.175	$75.8^{+1.2}_{-1.3}$	556^{+175}_{-172}	$8.38^{+0.75}_{-0.71}$	$9.04^{+0.45}_{-0.46}$
(c)	Incoming	1.636	$9.0^{+2.8}_{-2.8}$	3460^{+27}_{-15}	$2.08^{+0.01}_{-0.02}$	$7.10^{+0.00}_{-0.01}$
(d)	Outgoing	2.374	$9.0^{+2.9}_{-2.8}$	3430^{+31}_{-22}	$2.08^{+0.02}_{-0.02}$	$6.75^{+0.00}_{-0.01}$
(e)	Outgoing	2.854	$67.5^{+0.2}_{-0.4}$	583^{+181}_{-179}	$5.36^{+0.04}_{-0.09}$	$5.65^{+0.12}_{-0.11}$
(f)	Incoming	3.141	$64.4^{+1.1}_{-1.4}$	598^{+192}_{-187}	$4.74^{+0.21}_{-0.23}$	$4.98^{+0.09}_{-0.07}$
(g)	Incoming	3.523	$10.3^{+3.4}_{-3.2}$	3008^{+33}_{-35}	$2.08^{+0.03}_{-0.01}$	$4.48^{+0.01}_{-0.00}$

Figure 6 shows that A399 and A401 are very likely to be gravitationally bound unless the projection angle α is smaller than 7° . An unbound orbit would require a true relative velocity $V > 4400$ km s $^{-1}$, which will lead to a very quick separation of the clusters. We should assume that we are not viewing the cluster system at such a special time when the projected separation rate reaches more than $4 h^{-1}$ Mpc per Gyr for a pair of clusters only $2.05 h^{-1}$ Mpc apart.

For cases (d) and (g), the present relative velocity of this bound system *exceeds* the physical velocity dispersion within each cluster, and the clusters are so close together that they should have begun to coalesce or have just coalesced. If the system was at such evolutionary situation, we would expect to see some strong merging distortion between these two clusters in the X-ray surface brightness contours, contrary to the *ROSAT* PSPC image in fig. 1 of Fabian et al. (1997). Therefore, these two solutions can be definitely ruled out.

Cases (e) and (f) are two solutions with larger projection angles, but their dynamical states are different. Case (e) is an expanding (outgoing) model in which the last encounter event occurred about $2.5 h^{-1}$ Gyr ago, and the cluster pair will expand for another $1.0 h^{-1}$ Gyr, reaching a maximum extent of $5.65 h^{-1}$ Mpc. The true relative velocity is 583 km s $^{-1}$, and the two clusters are $\sim 5.4 h^{-1}$ Mpc apart along the direction with a projection angle of 67.5° . A collapsing model defined in case (f) is also allowed for this system. According to this model, the two clusters passed through each other $3.7 h^{-1}$ Gyr ago, and reached the last maximum expansion of $5.0 h^{-1}$ Mpc about $0.8 h^{-1}$ Gyr ago.

It is rather hard to determine whether the system is collapsing or expanding at present. The high resolution observations by the *XMM-Newton* observatory confirmed the enhancement in X-ray flux and temperature in the region between the two clusters, but no clues of intracluster compression or shock wave were found (Sakelliou & Ponman 2004). Gastaldello et al. (2003)

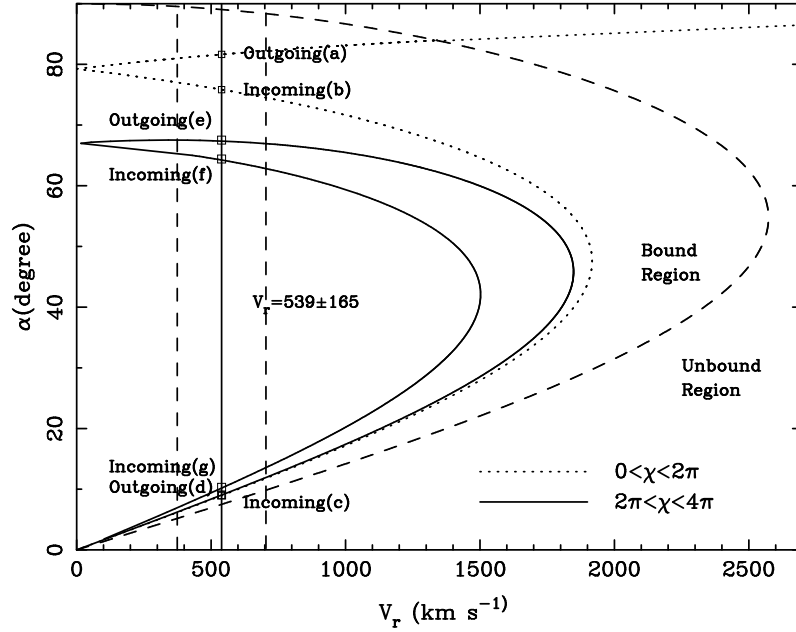


Fig. 6 Projection angle α as a function of relative radial velocity V_r predicted by the two-body model. Four bound solutions are presented at $V_r = 539 \pm 165 \text{ km s}^{-1}$ within $2\pi < \chi < 4\pi$. The limit between the bound and unbound regions is also given.

pointed out that the profiles of X-ray surface brightness, temperature and metallicity will shed light on the large-scale dynamics of the binary cluster system. Sakelliou & Ponman (2004) presented a clear contour plot of the residual smoothed images for these two clusters (see figure 6 therein) where positive residuals can be found to the south-west of the central cD galaxy in A401 as well as to the north of the one in A399. This indicates that A401 is moving from the south-west to the north-east while A399 is moving to the south. This feature seems to favor the scenario in which this pair of clusters is currently expanding. Since the projection angles are 67.5° in case (e), we can not expect to see a significant azimuthally asymmetric surface brightness for each cluster in the *ROSAT* PSPC brightness contour maps of this cluster pair (see figure 2 in Markevitch et al. 1998). However, a steeper gradient is marginally detectable in the north-east part of A401, and this also points toward an expanding picture. Therefore, case (e) is the more likely solution of the two-body model.

It should be noted that the two-body model disregards any angular momentum of the system, and it ignores the distribution of the matter within individual clusters which will be important when the two clusters are close to merger. The gravitational interaction from the matter outside the cluster pair is also neglected. It is well appreciated that dark matter mass dominates in the overall dynamical mass of individual clusters. Since our estimate of dynamical mass is based on the virial theorem, the two-body model assumes that the dark matter within a cluster is in approximate virial equilibrium. Despite the above-mentioned restrictions, the two-body model still provides a concise approach which is widely used to discuss the dynamic state of some gravitationally bound systems.

5 SUMMARY

We have investigated the dynamics of the cluster pair A399/A401, using the existing redshift measurements. We applied the KMM algorithm on a sample of 215 galaxies with known radial velocities, and obtained a robust separation of this cluster pair. Based on the velocity structure and virial mass estimate of the individual clusters, we explored the two-body model for studying the merger dynamics between them. Because the observational features in the radio and X-ray wavebands suggest that this pair of clusters have once experienced a close encounter, we derived four gravitationally bound solutions within the range of χ between 2π and 4π . The recent X-ray data from the *ROSAT* and *XMM-Newton* observations can be used to choose the most likely two-body model, according to which the pair of clusters has a true separation of $5.4 h^{-1}$ Mpc, is currently expanding at 583 km s^{-1} along a direction with a projection angle of 67.5° , and will reach a maximum extent of $5.65 h^{-1}$ Mpc in about $1.0 h^{-1}$ Gyr.

Acknowledgements We thank the anonymous referee for his helpful comments. This work is supported by the National Key Base Sciences Research Foundation under contract G1999075402, and the National Natural Science Foundation of China through grant 10273007.

References

- Ashman K. M., Bird C. M., Zepf S. E., 1994, *AJ*, 108, 2348
Bautz L., Morgan W., 1970, *ApJ*, 162, L149
Beers T. C., Geller M. J., Huchra J. P., 1982, *ApJ*, 257, 23
Beers T. C., Flynn K., Gebhardt K., 1990, *AJ*, 100, 32
Burns J. O., Roettiger K., Ledlow M. et al., 1994, *ApJ*, 427, L87
Burns J. O., Loken C., Gomez P. et al., 1997, In: N. Soker, ed., *ASP Conf. Ser. Vol. 115, Cooling Flows in Galaxies and Clusters*, San Francisco: ASP, p.21
Colless M., Dunn A. M., 1996, *ApJ*, 458, 435
Edge A. C., Stewart G. C., Fabian A. C., 1992, *MNRAS*, 258, 177
Fabian A. C., Peres C. B., White D. A., 1997, *MNRAS*, 285, L35
Fujita Y., Koyama K., Tsuru T. et al., 1996, *PASJ*, 48, 191
Harris D. E., Kapahi V. K., Ekers R. D., 1980, *A&AS*, 39, 215
Hill J. M., Oegerle W. R., 1993, *AJ*, 106, 831
Gastaldello F., Ettori S., Molendi S. et al., 2003, *A&A*, 411, 21
Geller M. J., Peebles P. J. E., 1973, *ApJ*, 184, 329
Markevitch M. et al., 1998, *ApJ*, 503, 77
McGlynn T. A., Fabian A. C., 1984, *MNRAS*, 208, 709
Nemec J. M., Nemec A. F. L., 1993, *AJ*, 105, 1455
Oegerle W. R., Hill J. M., 1994, *AJ*, 107, 857
Oegerle W. R., Hill J. M., 2001, *AJ*, 122, 2858
Sakelliou I., Ponman T. J., 2004, *MNRAS*, 351, 1439
White S. D. M., 1976, *MNRAS*, 177, 717
White S. D. M., Briel U. G., Henry J. P., 1993, *MNRAS*, 261, L8